IEEE Sensors Council

Theoretical Study on the Role of Gating and Photoconduction on Ga_2O_3 Phototransistors

Chuankai Hu, Peng Li, Longpu Wang, Siqi Li, Bowen Lv, Yanjie Wang, and Jiangang Ma

***Abstract*—Gallium oxide (Ga_2O_3) phototransistors with low dark current and high ON-OFF ratio have been attracting considerable attention for UV-C light detection applications. However, the joint influence of photoconduction and gating on their photoresponse behaviors makes the photodetection mechanism experimentally ambiguous. Herein, a theoretical study on Ga_2O_3 phototransistors is performed with technology computer-aided design (TCAD) Silvaco software to reveal the role of gate bias and external UV-C light illumination on their electrical characteristics. The analyses on the transfer curves before and after 250-nm light illumination figure out that the responsivity increases and then decreases with the gate bias, and the gate bias required to achieve the maximum responsivity increases with Ga_2O_3 thickness. Interestingly, under weak light irradiation, the current density of Ga_2O_3 phototransistors is found to be obviously enhanced by the gate bias owing to the effective separation of photo-generated electron-hole pairs. However, this gating effect is weakened upon strong UV-C light illumination. Our theoretical work clarifies the synergism and competition relationships between photoconduction and gating effects and offers a reference for the design of high-performance Ga_2O_3 phototransistors.**

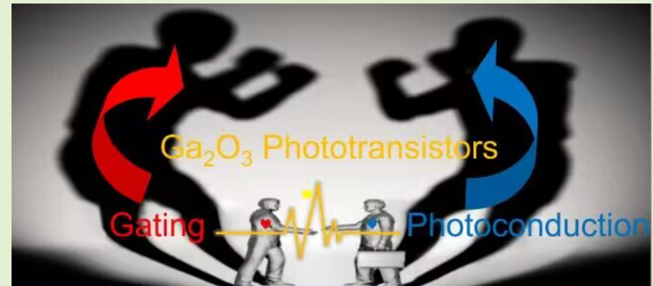

***Index Terms*—Gallium oxide (Ga_2O_3), gating, photoconduction, phototransistor, responsivity, UV-C light detection.**

I. Introduction

GALLIUM oxide (Ga_2O_3) has a large band gap, tunable electron concentration, high solar-blind light absorption coefficient, and excellent stability toward temperature, radiation, and electric field, and thus has been attracting much attention from the academic and industry communities [1], [2], [3], [4], [5]. Especially, Ga_2O_3 phototransistors with large ON-OFF current ratio and high responsivity show great potential for UV-C photodetection which are widely used in the military and civilian fields such as missile guidance, environmental monitoring, and short distance secure communication [6]. In the recent decade, various fabrication and characterization techniques have been used to study the physical properties of Ga_2O_3 material and devices [7], [8], [9], [10]. The performance of Ga_2O_3 phototransistors has been enhanced remarkably via the optimization of crystalline quality and the design of device configuration. For example, Liu et al. [11] fabricated a Ga_2O_3 nanosheet based phototransistor that exhibited a dark current of 5 pA, the ON-OFF ratio of 10^6, the responsivity of 4.79×10^5 A/W, and a decay time of about 25 ms.

Although great progress has been made toward high-performance Ga_2O_3 phototransistors, the modulation mechanism of the gate voltage (V_{GS}) remains ambiguous. On the dark condition, the transfer characteristic curves of Ga_2O_3 phototransistors can be turned from OFF-state to subthreshold region, to linear region, and then to fully ON-state with the increase of V_{GS}. Once the UV-C light is illuminated, the electron concentration in Ga_2O_3 increases and the threshold voltage decreases [12]. Then, the drain current (I_D) will be controlled by the thickness of the Ga_2O_3 film, the V_{GS}, and the illuminated light intensity, which arouses some questions as follows:

1) Are there optimal Ga_2O_3 thickness and V_{GS} that can balance the UV-C light absorption and carrier transport controllability?
2) How to distinguish the contribution and take full advantages of photoconduction and gating effects to the I_D?

Although a few pioneering experimental works have studied the UV-C light intensity- and V_{GS}-dependent response of

Manuscript received 9 September 2023; accepted 26 September 2023. Date of publication 5 October 2023; date of current version 14 November 2023. This work was supported in part by the National Key Research and Development Program under Grant 2021YFA0716404, in part by the 111 Project under Grant B13013, in part by the Jilin Province under Grant 2022C040-1, and in part by the Fundamental Research Funds for the Central Universities. The associate editor coordinating the review of this article and approving it for publication was Prof. Hsin-Ying Lee. *(Corresponding authors: Peng Li; Jiangang Ma.)*

Chuankai Hu, Peng Li, Longpu Wang, Siqi Li, Bowen Lv, and Jiangang Ma are with the Key Laboratory of UV-Emitting Materials and Technology of Ministry of Education, Northeast Normal University, Changchun 130024, China (e-mail: lip032@nenu.edu.cn; majg@nenu.edu.cn).

Yanjie Wang is with the Laboratory for Comprehensive Energy Saving of Cold Regions Architecture of Ministry of Education, School of Electrical Engineering and Computer, Jilin Jianzhu University, Changchun 130118, China.

This article has supplementary downloadable material available at https://doi.org/10.1109/JSEN.2023.3320797, provided by the authors.

Digital Object Identifier 10.1109/JSEN.2023.3320797

1558-1748 © 2023 IEEE. Personal use is permitted, but republication/redistribution requires IEEE permission.
See https://www.ieee.org/publications/rights/index.html for more information.

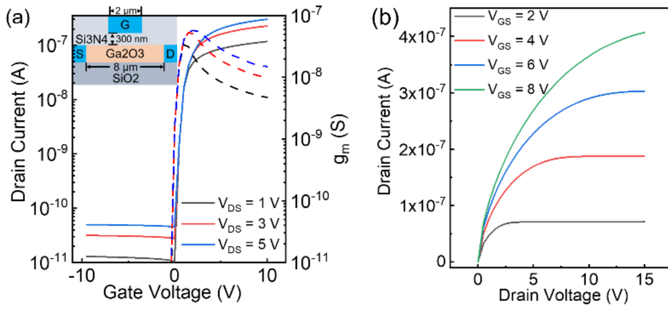

Fig. 1. (a) Transfer characteristic curves at different drain voltages. Inset is the structure schematic of the Ga_2O_3 phototransistor. (b) Output characteristic curves at different gate voltages.

Ga_2O_3 phototransistors [13], there is no consensus due to the complex and interrelated relationship between gating and photoconduction, along with the difficulties in systematically screening extensive experimental parameters.

Numerical simulation can complement the experimental data and is suitable for mechanism analyses owing to the controllable parameter variation and visual current density. However, the theoretical study of the emerging wide bandgap semiconductor, Ga_2O_3 is rare up to date [14]. Given that technology computer-aided design (TCAD) Silvaco is mature software in the semiconductor industry that can be used for simulating the field effect transistors (FETs) and diodes [15], this work reports the theoretical study of Ga_2O_3 phototransistors that clarifies the evolution rule of Ga_2O_3 thickness- and V_{GS}-dependent responsivity. Importantly, the simulations of current density under a wide range of V_{GS} and continuously variable light intensity enable the revelation of photoconduction and gating impacts on the photoresponse behavior of Ga_2O_3 phototransistors.

II. Simulation Method of Ga_2O_3 Phototransistors

The Ga_2O_3 phototransistors have a top-gate structure consisting of SiO_2 substrate, Ga_2O_3 channel, Si_3N_4 dielectric layer, source and drain electrodes with a work function of 4.6 eV, and a top gate electrode with a work function of 5.0 eV. The structure parameters of the device are shown in the inset of Fig. 1(a) and the defined parameters of Ga_2O_3 are shown in Table I [16], [17], [18]. In the code, Ga_2O_3 is n-type and has traps. Ga_2O_3 material has interface defects and body defects. In this article, the trap is set to be studied as a body defect. The transfer characteristics have been studied by varying the mobility of the electrons and holes. The results show that the mobility of holes does not affect the curves, indicating that the traps within the Ga_2O_3 bind the holes.

The models used in the simulation include the drift-diffusion, carrier mobility, trap, etc. The drift-diffusion model mainly consists of three equations: Poisson's, carrier continuity, and carrier transport [19]. ψ is the electrostatic potential, ε is the local dielectric constant, ρ is the local space charge density, J_n is the current density of the electrons, q is the magnitude of the charge on the electrons, J_n is the electron mobility, D_n is the diffusion coefficient of the electrons, n is the concentration of the electrons, G_n is the rate of generation of electrons, and R_n is the electron complexation rate

TABLE I
Parameters of Ga_2O_3 Used in the Simulation

Affinity	4.0 eV
Band gap	4.8 eV
Density of conduction band states	3.72×10^{18}
Density of valence band states	3.72×10^{18}
Dielectric constant	10.0 $C^2/(N{\cdot}M^2)$
Thermal conductivity	0.13 W/(m·K)
Electron mobility	118 $cm^2/(V{\cdot}s)$
Hole mobility	0.1 $cm^2/(V{\cdot}s)$
Trap energy level (From conduction band)	0.6 eV
Trap density	1×10^{16} cm^{-3}
Electron capturing cross-sections	6.6×10^{-14} cm^{-2}
Hole capturing cross-sections	1×10^{-20} cm^{-2}

Poisson equation: $\mathrm{div}(\varepsilon \nabla \psi) = -\rho$
electron transport equation: $\vec{J}_n = q\mu_n \vec{E}_n n + qD_n \vec{\nabla}_n$
electron continuity equation: $\partial n/\partial t = 1/q \vec{\nabla} \cdot \vec{J}_n + G_n - R_n$.

The mobility model is a critical model that affects the accuracy of device modeling. There is more than one scattering mechanism for the mobility of Ga_2O_3 transistors. The following focuses on the bulk mobility model used [20]

$$\mu_{\mathrm{const}} = 118 \times \left(\frac{T}{300\mathrm{K}}\right)^{-1.5}.$$

In the trap model, the trap cross-sectional area significantly affects the rate at which the trap captures carriers, and variation of this parameter will have a corresponding effect on the lifetime of the minority carrier in some regions of the material, as shown in the following equation. N_{trap} is the trap density, v_{th} is the carrier saturation rate, and σ is the trap cross-sectional area [21]

$$\tau_{\mathrm{trap}} = \frac{1}{N_{\mathrm{trap}} v_{\mathrm{th}} \sigma} \exp\left(\frac{E_c - E_{\mathrm{trap}}}{kT}\right).$$

The transfer and output curves of the 100 nm thick Ga_2O_3 phototransistor are shown in Fig. 1(a) and (b), respectively. The right y-axis is shown to describe the relationship between g_m and V_{GS} [22] so that the different areas of the device can be distinguished. The transfer characteristic curves under different V_{DS} show significant rectification behavior with an ON-OFF ratio of about 10^4 and a turn-on voltage of 0 V. The output characteristic curves exhibit linear and saturation regions as the V_{DS} increases. The simulated electrical properties are consistent with the experimental transfer and output curves of Ga_2O_3 FETs [23] and thus lay a foundation for the following investigation.

III. UV-C Photodetection Performance Modulation

The light absorption characteristic of Ga_2O_3 is crucial for their photodetection performance and thus is studied at first. As shown in Fig. 2(a), the absorptivity of Ga_2O_3 gradually increased with the wavelength decreases from 400 to 200 nm, and strong absorption is achieved in the UV region. We observed that the intersection of the blue tangent line with

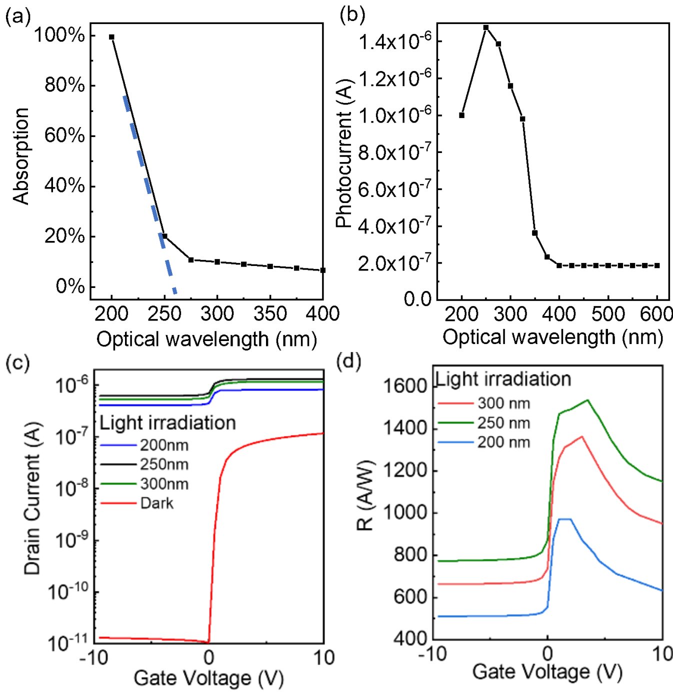

Fig. 2. (a) Simulated light absorptivity of 100 nm Ga_2O_3 film changes with the wavelengths of light. (b) Saturated photocurrent of Ga_2O_3 phototransistor at different incident light wavelengths, the 250 nm light intensity is 1 μW/cm^2 and the V_{DS} = 3 V. (c) Transfer characteristic curves with different wavelengths of light irradiation, the light intensity is 1 μW/cm^2, and the V_{DS} = 3 V. (d) V_{GS}-dependent responsivity with different wavelengths of light irradiation.

the x-axis in the figure is about 260 nm, and we calculated that Eg is about 4.8 eV. Fig. 2(b) shows the photocurrent of the Ga_2O_3 phototransistor change with the wavelength of incident light. The highest photocurrent was obtained at the wavelength around 250 nm, which consists well with the bandgap of Ga_2O_3. The transfer characteristic curves at dark and at incident light wavelengths of 200, 250, and 300 nm are shown in Fig. 2(c). The corresponding responsivity changing with V_{GS} is shown in Fig. 2(d). The responsivity (R) is obtained according to the equation $R = (I_{\text{light}} - I_{\text{dark}})/(P_{\text{light}} S)$, where I_{light} and I_{dark} represent the current recorded with and without light irradiation, P_{light} is the power density of light, and S is the area of the channel [24]. The responsivity of Ga_2O_3 phototransistors increases sharply in the threshold region and reaches the highest value in the initial ON-state of the device. Additionally, the strongest photoresponse behavior occurs at 250 nm which agrees with the change of photocurrent with light wavelength.

The V_{GS}-dependent photodetection performance of Ga_2O_3 phototransistors with different Ga_2O_3 thicknesses was studied. As shown in Fig. 3(a)–(e), under 254 nm wavelength light irradiation, the transfer curve moves upward for about one magnitude while $V_{GS} > 2$ V and for more than four magnitudes while $V_{GS} < 0$ V. These light response behaviors are consistent with experimental light detection results [11] and confirm the accuracy of our theoretical simulation. When 254 nm light is applied, a large number of photogenerated carriers are produced which will participate in the conduction. As a result, the ON/OFF ratio in the OFF-state is several orders

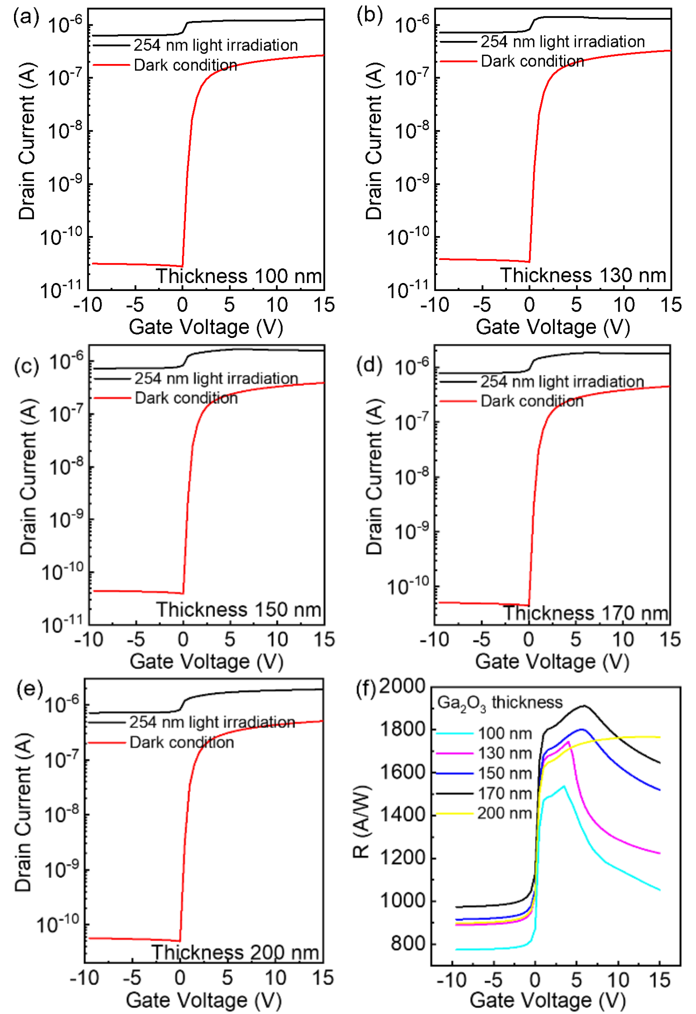

Fig. 3. (a)–(e) Transfer characteristic curves with and without 250 nm light irradiation. (f) V_{GS}-dependent responsivity (R) with different Ga_2O_3 thicknesses. In (a)–(e), the 250 nm light intensity is 1 μW/cm^2 and the V_{DS} = 3 V.

of magnitude higher than in the ON-state. We calculated the V_{GS}-dependent responsivity with Ga_2O_3 thickness ranging from 100 to 200 nm. In Fig. 3(f), when the thickness is constant, the responsivity first increases slowly, then increases rapidly, and finally decreases. The variation tendency of R under different V_{GS} is determined by the difference between I_{light} and I_{dark}. At high V_{GS}, the decrease in R is ascribable to the faster increase rate of I_{dark}. Furthermore, the max R first increases and then decreases with the increase of Ga_2O_3 thickness. This is caused by the trade-off between the light absorption and the gate control [25]. The light absorption efficiency increases with the channel thickness whereas the gate control is weakened.

From Fig. 3(f), the article also finds out that the responsivity of the Ga_2O_3 phototransistors finally decreases with the V_{GS} increasing when the thickness of the Ga_2O_3 layer is lower than 170 nm. This is because as the number of intrinsic carriers increases with thickness, the increase in V_{GS} causes the gate electrode to attract more intrinsic carriers, increasing dark current. However, due to the significant decrease in absorption of the thinner Ga_2O_3 layer, the number of photogenerated carriers is limited, resulting in trivial changes in photocurrent

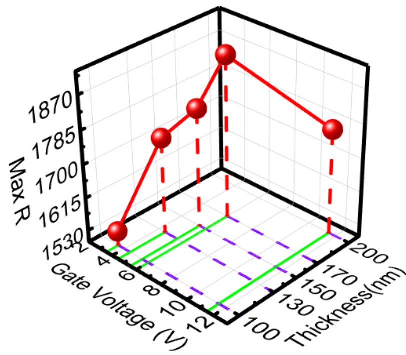

Fig. 4. Relationship between maximum responsiveness, gate voltage, and thickness.

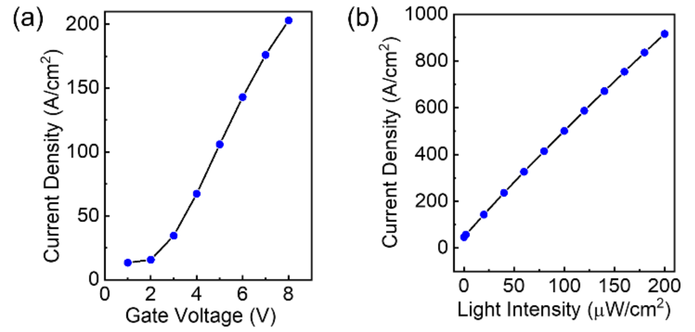

Fig. 5. (a) Maximum total current density under 250 nm light irradiation when the light intensity is 1 μW/cm^2. (b) Maximum total current density for different light intensities when $V_{GS} = 6$ V.

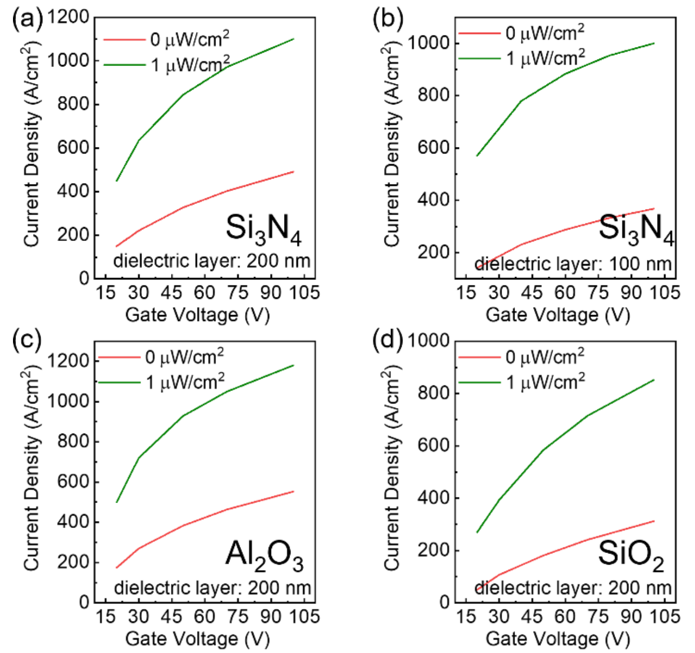

Fig. 6. Total current density as a function of gate voltage. Si_3N_4 dielectric layer thickness is 200 nm (a) and dielectric layer thickness is 100 nm (b). Al_2O_3 dielectric layer thickness is 200 nm (c) and SiO_2 dielectric layer thickness is 200 nm (d). The Ga_2O_3 thickness is 170 nm and the $V_{DS} = 3$ V.

with increasing V_{GS}. In contrast, when the thickness of the Ga_2O_3 layer is 200 nm, the responsivity does not appear to decrease. This is due to the simultaneously increased number of photogenerated carriers, making the light current match the increase in dark current. Therefore, the responsivity curve remains relatively flat with the V_{GS} increasing. More interestingly, as shown in Fig. 4, the maximum R increases and then decreases as the thickness increases. The V_{GS} corresponding to the maximum R increases and shifts to the right. These observations indicate that the combined effect of photoconduction and gating determines the photoresponse behaviors. Based on the above results, the parameters at the highest responsivity were chosen for better results in subsequent experiments. The thickness is 170 nm and the V_{GS} is 6 V.

IV. Role of Gating and Photoconduction

Photoconduction is defined to describe the enhancement in I_D under a fixed V_{DS} by the photo-generated carriers [26]. The photoconduction is modulated by the gating because once a V_{GS} higher than the threshold voltage is applied, the carrier distribution changes and the conduction channel forms at the Ga_2O_3/gate dielectric interface, and thus, the photoconduction is weakened. To verify this, the total current density of the Ga_2O_3 phototransistors changing with V_{GS} and light intensity was investigated, as shown in Fig. 5(a) and (b). The current density was used as a study indicator rather than current to make the results more intuitive and comparable. As the gate voltage or light intensity increases, the maximum total current density increases, indicating that the gating or photoconductance effect plays an increasingly strong role.

To properly regulate the gating, we test different dielectric layer thicknesses and dielectric layer materials. As shown in Fig. 6(a) and (b), as the thickness is reduced, the curves become parallel earlier, indicating that this operation effectively improves the gating effect. Similarly, different dielectric layer materials also affect the distribution of electric field lines due to their different dielectric constants, which ultimately leads to varying levels of attraction to carriers in the channel. As shown in Fig. 6(c) and (d), we changed the dielectric materials to Al_2O_3 and SiO_2 and found that the change in the curves of the Al_2O_3 material is not apparent. The current density in the curves of the SiO_2 material is reduced, and the curves reach parallel later. This is because the dielectric constant size of Si_3N_4 and Al_2O_3 are about 7, so the capacitance is similar to the identical results. The dielectric layer material of Si_3N_4 and a thickness of 100 nm were selected for the subsequent studies in this article.

To further reveal the interaction between gating and photoconduction and their impacts on the photoresponse behaviors, we simulated the current density in the Ga_2O_3 channel layer in the following circumstances: 1) under different UV-C light intensities with V_{GS} of zero; 2) under different UV-C light intensities and a constant V_{GS} of 6 V; 3) under different V_{GS}; and 4) under different V_{GS} and constant UV-C light intensity. For cases 1 and 2, the simulated total current density as a function of UV-C light intensity is illustrated in Fig. 7(a). When no gate voltage is applied, the number of photogenerated carriers increases with the light intensity, and the slope is nearly stable. Under V_{GS}, the current density at the same light intensity becomes higher. At high light intensities ($\geq$30 μW/cm^2), the difference in current density between

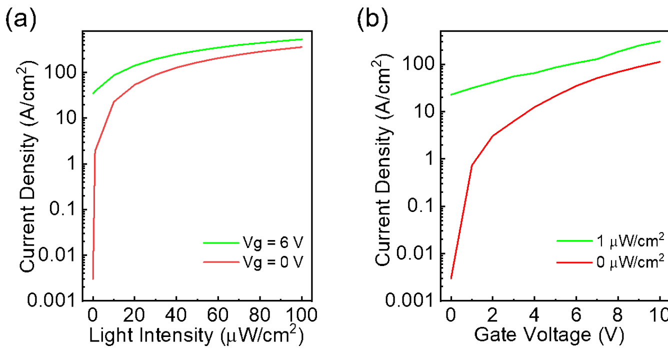

Fig. 7. Logarithmic total current density as a function of UV-C light intensity (a) and gate voltage (b). The Ga_2O_3 thickness is 170 nm and the $V_{DS} = 3$ V.

cases 1 and 2 is small, indicating that the gating effect is weakened.

For cases 3 and 4, the simulated total current density as a function of V_{GS} is illustrated in Fig. 7(b). Without UV-C light illumination, the current density increases rapidly at low V_{GS} region and slowly in the high V_{GS} region due to the finite number of intrinsic free carriers in the Ga_2O_3 channel layer [27]. After UV-C light is applied, the current density increases sharply owing to the contribution of photo-generated carriers. As V_{GS} increases further, the current density curves are parallel. This is because the photogenerated carriers are all attracted by the high V_{GS} (≥ 8 V). The attracted intrinsic carriers with increasing V_{GS} eventually contribute to the current density, thus leading to an equal slope. Based on the above observations, the competitive relationship between gating and photoconductivity can be summed up as the gate control under weak light and the photoconduction dominates under strong light. On the other hand, the theoretical simulation has the advantage of performing extreme conditions that are difficult to achieve in experiments but could provide a reference for experimental study. For instance, operating voltages (V_{GS}) above 500 V were performed to check the current density change tendency. The results are consistent with those shown in Fig. 7(b). Furthermore, similar gating control can be obtained at lower V_{GS} by decreasing the dielectric layer thickness.

According to our current density distribution simulations, a synergistic relationship was also observed from the above competing. As shown in Fig. 8(a)–(c), the current density of the Ga_2O_3 phototransistor under both V_{GS} and UV-C light illumination is much higher than the sum of those under only V_{GS} and only UV-C light illumination. As the mechanism schematics shown in Fig. 8(d)–(f), gate voltage can attract a small number of free electrons from the Ga_2O_3 layer and make them accumulate at the Ga_2O_3/dielectric layer to form a conduction channel [28]. Under UV-C light irradiation, some of the photo-generated electrons and holes will participate in conduction with the others recombine before being collected by the source and drain electrodes [29]. In contrast, if both V_{GS} and UV-C light are applied, the recombination of photo-generated electrons and holes will be suppressed because of the vertical gate electric field-driven space separation. The photo-generated electrons will be more efficiently collected by the source and drain electrodes. When exposed

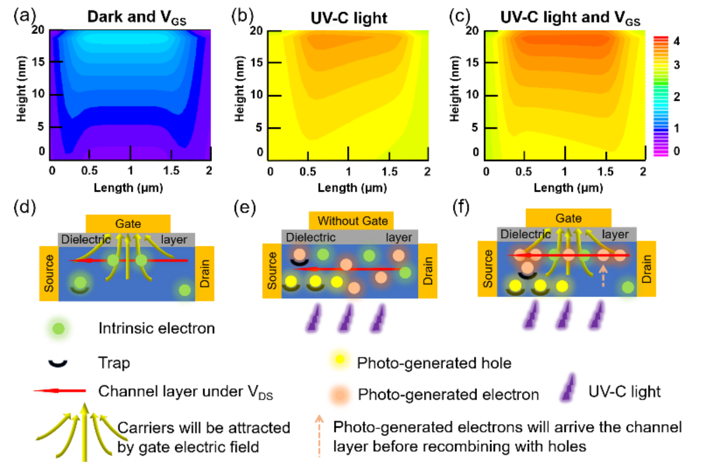

Fig. 8. Logarithmic current density distribution and corresponding mechanism schematic of the Ga_2O_3 phototransistors obtained under (a) and (b) only $V_{GS} = 6$ V, (b) and (e) only 100 μW/cm^2 UV-C light, and (c) and (f) both $V_{GS} = 6$ V and 100 μW/cm^2 UV-C light. The V_{DS} is 3 V for (a) and (c), and the region in (a)–(c) are selected from the center of the Ga_2O_3 channel beneath the gate electrode. The light source is located under the substrate. The direction of light incidence is below the substrate. The source and drain electrodes are on the left and right sides, respectively.

to UV-C light, traps in the material capture photo-generated carriers and mainly photo-generated holes. Therefore, higher current density is achieved, and better photodetection performance than the two-terminal devices could be realized. Additionally, similar results were obtained in aluminum gallium nitride (AlGaN) based devices, suggesting that our simulation method and proposed mechanism are applicable to other semiconductor-based phototransistors.

According to the simulation results, the UV detection capability of the Ga_2O_3 phototransistor can be applied in the fields of UV guidance, missile warning, fire warning, and environmental detection. Yoon et al. [30] examined the impact of light and gate voltage on the device. They produced β-Ga_2O_3 synaptic FETs with Sn doping, which imitate optical and electrical spike stimulation. In biomimicry, our work has the role of advancing neuromorphic computing in the future.

V. Conclusion

In summary, the UV-C photodetection performance of Ga_2O_3 phototransistors was simulated with TCAD. We found that the thickness of the Ga_2O_3 channel layer plays a crucial role in balancing the trade-off between the UV-C light absorption efficiency and gate control function. Further, the gate voltage required to achieve the maximal responsivity should be adjusted to match the thickness of the Ga_2O_3 channel. The gate voltage- and UV-C light intensity-dependent current density analyses figure out that the photoresponse behaviors of Ga_2O_3 phototransistors are determined by the synergism and competition between the photoconduction and gating effects, which dominate under strong and weak light irradiation conditions, respectively. Our theoretical simulation provides a reference for the experimental design of high-performance Ga_2O_3 phototransistors and offers profound insights into their UV-C photodetection mechanism. The simulation results have also been verified to be valid for other semiconductor photoresistors.

References

[1] J. Y. Tsao et al., "Ultrawide-bandgap semiconductors: Research opportunities and challenges," *Adv. Electron. Mater.*, vol. 4, no. 1, Jan. 2018, Art. no. 1600501, doi: 10.1002/aelm.201600501.

[2] Z. Yang et al., "Deep UV transparent conductive Si-doped Ga_2O_3 thin films grown on Al_2O_3 substrates," *Appl. Phys. Lett.*, vol. 122, no. 17, Apr. 2023, Art. no. 172102, doi: 10.1063/5.0147004.

[3] J. Zhang et al., "Ultra-wide bandgap semiconductor Ga_2O_3 power diodes," *Nature Commun.*, vol. 13, no. 1, pp. 1723–2041, Jul. 2022, doi: 10.1038/S41467-022-31664-Y.

[4] H. Sheoran, V. Kumar, and R. Singh, "A comprehensive review on recent developments in ohmic and Schottky contacts on Ga_2O_3 for device applications," *ACS Appl. Electron. Mater.*, vol. 4, no. 6, pp. 2589–2628, Jun. 2022, doi: 10.1021/acsaelm.2c00101.

[5] N. Manikanthababu et al., "Electrical characteristics and defect dynamics induced by swift heavy ion irradiation in Pt/PtO/-Ga_2O_3 vertical Schottky barrier diodes," *IEEE Trans. Electron Devices*, vol. 69, no. 11, pp. 5996–6001, Nov. 2022, doi: 10.1109/TED.2022.3207702.

[6] H. Yoo, I. S. Lee, S. Jung, S. M. Rho, B. H. Kang, and H. J. Kim, "A review of phototransistors using metal oxide semiconductors: Research progress and future directions," *Adv. Mater.*, vol. 33, no. 47, Nov. 2021, Art. no. 2006091, doi: 10.1002/adma.202006091.

[7] W. Kong et al., "Graphene-β-Ga_2O_3 heterojunction for highly sensitive deep UV photodetector application," *Adv. Mater.*, vol. 28, no. 48, pp. 10725–10731, Dec. 2016, doi: 10.1002/adma.201604049.

[8] Z. Hu et al., "Enhancement-mode Ga_2O_3 vertical transistors with breakdown voltage >1 kV," *IEEE Electron Device Lett.*, vol. 39, no. 6, pp. 869–872, Jun. 2018, doi: 10.1109/LED.2018.2830184.

[9] T.-S. Chou et al., "Suppression of particle formation by gas-phase prereactions in (100) MOVPE-grown β-Ga_2O_3 films for vertical device application," *Appl. Phys. Lett.*, vol. 122, no. 5, p. 6951, Jan. 2023, doi: 10.1063/5.0133589.

[10] B. R. Tak et al., "Recent advances in the growth of gallium oxide thin films employing various growth techniques—A review," *J. Phys. D, Appl. Phys.*, vol. 54, no. 45, Nov. 2021, Art. no. 453002, doi: 10.1088/1361-6463/ac1af2.

[11] Y. Liu et al., "Ga_2O_3 field-effect-transistor-based solar-blind photodetector with fast response and high photo-to-dark current ratio," *IEEE Electron Device Lett.*, vol. 39, no. 11, pp. 1696–1699, Nov. 2018, doi: 10.1109/LED.2018.2872017.

[12] Y. Qin et al., "Enhancement-mode β-Ga_2O_3 metal–oxide–semiconductor field-effect solar-blind phototransistor with ultrahigh detectivity and photo-to-dark current ratio," *IEEE Electron Device Lett.*, vol. 40, no. 5, pp. 742–745, May 2019, doi: 10.1109/LED.2019.2908948.

[13] P. Tan et al., "Hysteresis-free Ga_2O_3 solar-blind phototransistor modulated from photoconduction to photogating effect," *Appl. Phys. Lett.*, vol. 120, no. 7, Feb. 2022, Art. no. 071106, doi: 10.1063/5.0078904.

[14] M. Khurana, Upasana, M. Saxena, and M. Gupta, "Highly sensitive Ga_2O_3-face tunnel field effect phototransistor for deep UV detection," *IEEE Sensors J.*, vol. 22, no. 18, pp. 17769–17776, Sep. 2022, doi: 10.1109/JSEN.2022.3194653.

[15] W. Lei et al., "Proposal and simulation of Ga_2O_3 MOSFET with PN heterojunction structure for high-performance E-mode operation," *IEEE Trans. Electron Devices*, vol. 69, no. 7, pp. 3617–3622, Jul. 2022, doi: 10.1109/TED.2022.3172919.

[16] Y. Qin et al., "Amorphous gallium oxide-based gate-tunable high-performance thin film phototransistor for solar-blind imaging," *Adv. Electron. Mater.*, vol. 5, no. 7, Jun. 2019, Art. no. 1900389, doi: 10.1002/aelm.201900389.

[17] S.-R. Min et al., "Analysis for DC and RF characteristics recessed-gate GaN MOSFET using stacked TiO_2/Si_3N_4 dual-layer insulator," *Materials*, vol. 15, no. 3, p. 819, Jan. 2022, doi: 10.3390/ma15030819.

[18] X. Zhou et al., "Realizing high-performance β-Ga_2O_3 MOSFET by using variation of lateral doping: A TCAD study," *IEEE Trans. Electron Devices*, vol. 68, no. 4, pp. 1501–1506, Apr. 2021, doi: 10.1109/TED.2021.3056326.

[19] K. Song et al., "Normally-off AlN/β-Ga_2O_3 field-effect transistors using polarization-induced doping," *J. Phys. D, Appl. Phys.*, vol. 53, no. 34, Aug. 2020, Art. no. 345107, doi: 10.1088/1361-6463/ab8d6e.

[20] M. H. Wong et al., "All-ion-implanted planar-gate current aperture vertical Ga_2O_3 MOSFETs with Mg-doped blocking layer," *Appl. Phys. Exp.*, vol. 11, no. 6, May 2018, Art. no. 064102, doi: 10.7567/APEX.11.064102.

[21] Z. Zhang, E. Farzana, A. R. Arehart, and S. A. Ringel, "Deep level defects throughout the bandgap of (010) β-Ga_2O_3 detected by optically and thermally stimulated defect spectroscopy," *Appl. Phys. Lett.*, vol. 108, no. 5, Feb. 2016, Art. no. 052105, doi: 10.1063/1.4941429.

[22] H. Sheoran et al., "High performance of zero-power-consumption MOCVD-grown β-Ga_2O_3-based solar-blind photodetectors with ultralow dark current and high-temperature functionalities," *ACS Appl. Mater. Interface*, vol. 14, no. 46, pp. 52096–52107, Nov. 2022, doi: 10.1021/acsami.2c08511.

[23] J. Ahn et al., "Ultrahigh deep-ultraviolet responsivity of a β-Ga_2O_3/MgO heterostructure-based phototransistor," *ACS Photon.*, vol. 8, no. 2, pp. 557–566, Jan. 2021, doi: 10.1021/acsphotonics.0c01579.

[24] X. Hou et al., "Ultrahigh-performance solar-blind photodetector based on α-phase-dominated Ga_2O_3 film with record low dark current of 81 fA," *IEEE Electron Device Lett.*, vol. 40, no. 9, pp. 1483–1486, Sep. 2019, doi: 10.1109/LED.2019.2932140.

[25] P. Li et al., "In_2O_3:Ni/Ga_2O_3 heterojunction thin-film transistors for UV-C photodetection," *IEEE Electron Device Lett.*, vol. 44, no. 3, pp. 432–435, Mar. 2023, doi: 10.1109/LED.2023.3238350.

[26] S. Kumar, S. Dhara, R. Agarwal, and R. Singh, "Study of photoconduction properties of CVD grown β-Ga_2O_3 nanowires," *J. Alloys Compounds*, vol. 683, pp. 143–148, Oct. 2016, doi: 10.1016/j.jallcom.2016.05.079.

[27] J. Ma, H. J. Cho, J. Heo, S. Kim, and G. Yoo, "Asymmetric double-gate β-Ga_2O_3 nanomembrane field-effect transistor for energy-efficient power devices," *Adv. Electron. Mater.*, vol. 5, no. 6, Jun. 2019, Art. no. 1800938, doi: 10.1002/aelm.201800938.

[28] M. Zhang et al., "Study of nonthermal-equilibrium carrier recombination and transport in β-Ga_2O_3 metal–semiconductor–metal deep-ultraviolet photodetectors," *IEEE Trans. Electron Devices*, vol. 70, no. 5, pp. 2336–2341, May 2023, doi: 10.1109/TED.2023.3253671.

[29] E. Li et al., "MXene based saturation organic vertical photoelectric transistors with low subthreshold swing," *Nature Commun.*, vol. 13, no. 1, p. 2898, May 2022, doi: 10.1038/s41467-022-30527-w.

[30] Y. Yoon, Y. Kim, W. S. Hwang, and M. Shin, "Biological UV photoreceptors-inspired Sn-doped polycrystalline β-Ga_2O_3 optoelectronic synaptic phototransistor for neuromorphic computing," *Adv. Electron. Mater.*, vol. 9, no. 7, Jul. 2023, Art. no. 2300098, doi: 10.1002/aelm.202300098.